

STM images of real (100) and (110) surfaces of tungsten and character of reflection of conduction electrons

S. L. Pryadkin and V. S. Tsoï

Institute of Solid Physics, USSR Academy of Sciences

(Submitted 23 July 1987)

Zh. Eksp. Teor. Fiz. **94**, 336–342 (March 1988)

Electrically polished (100) and (110) tungsten surfaces were investigated using a scanning tunnel microscope (STM) at atmospheric pressure. The (110) surface consists of large atomically-planar terraces, while the (100) surface is faceted. The STM data are used to explain the results of electron-focusing (EF) experiments, viz., the strong dependence of the probability of specular reflection of conduction electrons scattered by the (100) face on the de Broglie wavelength of the electrons, and the independence of the specular-reflection probability of the wavelength for the (110) surface.

Experiments have shown that a characteristic feature of conduction-electron reflection from the surface of a metal is the high probability of specular reflection at normal incidence. A high probability q of specular reflection was observed with the aid of transverse electron focusing¹ (EF) in W and Cu,² Ag,³ Zn,⁴ Al,⁵ Bi,¹ and Sb.⁶ The large values of q are evidence that an appreciable fraction of the real surface of a metal is perfect on an atomic scale (is atomically plane). In a number of cases, however, q exhibits a strong crystallographic anisotropy, and is most pronounced in tungsten.

Investigations^{8,9} of atomically smooth (100) and (110) faces of tungsten with the aid of the static skin effect⁷ have shown that the character of the conduction-electron reflection changes radically with change of the crystallographic orientation tungsten surface. The values obtained for the Fuchs parameter were $P = 0.6-0.8$ for the (110) face and $P = 0$ for the (100) face (diffuse scattering).

Measurements with the aid of the EF have shown that the specular-reflection probabilities of different groups of electrons from atomically smooth (100) and (110) tungsten surfaces agree, within experimental error, with the values for real surfaces that are saturated with adsorbed atoms and molecules. In the intermediate case, when the density of the adsorbed atoms is low, the probability of specular reflection decreases substantially.^{10,11} In the case of a real surface, the value of q for scattering by the (100) face depends strongly on the electron wavelength: $q = 0$ for electrons with a small de Broglie wavelength ($\lambda = 0.8 \text{ \AA}$), and electrons with large wavelengths (up to 50 \AA) are specularly reflected with high probability (up to 0.7). For a (110) surface, q is independent of the wavelength and amounts approximately to 0.6.

The decisive cause of the crystallographic anisotropy of q has not yet been determined. Alternate causes are the surface structure and the Fermi-surface geometry.

Many advances in the procedures for research into surface structure are due to the development of scanning tunnel microscopy (STM),¹² which makes it possible to determine, with atomic resolution, the structure of a real surface under normal conditions.¹³ The roughness parameters of a surface were determined by the STM method in Refs. 14 and 15. The structure of a real (100) surface of silicon was investigated in Ref. 14 under conditions of ordinary vacuum, while in Ref. 15 was investigated the structure of a polished silver surface [faces (100) and (110)] in ultrahigh vacuum

(10^{-10} Torr). In Ref. 15 the surface structure was investigated also with the aid of EF. By comparing the EF data with the character of the relief of the silver surface investigated with the aid of STM, the authors have shown that a "geometric-optics" description of the electron wave functions) is in good agreement with the EF experiment.

To establish the causes of the crystallographic anisotropy q in tungsten it is necessary to study the relief of the surface on a scale comparable with the conduction-electron de Broglie wavelength ($10-50 \text{ \AA}$). This was the purpose of the present study.

EXPERIMENT

The scanning tunnel microscope used to determine the surface relief had the following structural features and technical characteristics. A coarse-feed device of the differential-spring type (see Ref. 16) could feed the tungsten tip to the system from a distance on the order of $20 \mu\text{m}$ in steps of 100 \AA . An XYZ displacement pickup was made up of piezoelectric elements in the form of tubes. Provision was made in the pickup construction to compensate for the drift, due to thermal expansion of the ceramic, of the tip relative to the sample. A variant of such a compensation is described in Ref. 17. The maximum explored area was $3 \times 3 \mu\text{m}$ at field intensity less than 1 kV/cm in the piezoceramic. The displacements were graduated with an optical interferometer; the voltage-to-displacement conversion coefficients, accurate to 20%, were 50 \AA/V along Z and 150 \AA/V along X and Y . The experiments were performed at atmospheric pressure without thermal stabilization or acoustic shielding. The drift of the tip position relative to the sample was determined from the shift of the surface image in successive scanning cycle, and amounted approximately to 5 \AA/min at a room-temperature rate of change $2 \text{ }^\circ\text{C/h}$. The images were recorded with stabilized direct current through the tip ($\sim 3 \text{ nA}$) and at a reference voltage 100 mV . The scanning velocity was 100 \AA/s . The image noise, determined for atomically-flat sections of the surface, was 0.3 \AA (at frequencies $f < 10 \text{ Hz}$). The dependence of the current through the tip on its displacement was exponential with an effective electron work function $\varphi = 0.5-1 \text{ eV}$ (after contact of the tip with the sample surface). The (100) and (110) surfaces were investigated with one and the same tip. The data gathering and the reduction of the images were carried out with a MERA 1300

computer. In the data gathering regime, the computer controls the scanning and stores the data. The sample preparation method is described in Ref. 11. The bright-dipped samples were prepared immediately prior to the experiment with the STM.¹¹ Approximately 60 images were obtained. The tip was displaced several times in the course of the experiment by 1 mm relative to the sample.

RESULTS

Figures 1 and 2 show in different scales typical STM images of (100) and (110) tungsten surfaces. To assess the degree of roughness of the surface, we calculated the mean squared deviation $(\overline{\Delta h^2})^{1/2}$ relief from the median plane. In the reduced large images (2000–4000 Å) the mean squared deviation was the same for the faces (100) and (110) and amounted to 30–50 Å (Figs. 1a and 2b).

A feature of the (110) surface is the presence of large (500–1000 Å) atomically-flat sections in the (110) orientation, separated by drops of 20–100 Å (Fig. 1a). Figure 1b shows, with large magnification, a flat (110) section. The mean squared deviation from the median plane for Fig. 1b is 2.5 Å.

The (100) surface is faceted. The orientations of the surfaces of the facets can be easily determined from the greatly magnified picture in Fig. 2a. These are mainly faces of type {310} and faces intermediate between {310} and {100}. The mean squared deviation for the image in Fig. 2a is 8–10 Å. The characteristic facet sizes are 50–200 Å along the surface and 5–20 Å along the normal to it. Roughness of larger size are also encountered (with characteristic dimension 500 Å along the surface, see Fig. 2b).

Fourier spectra were calculated for images of surfaces larger than 1000 Å. For two variables we have

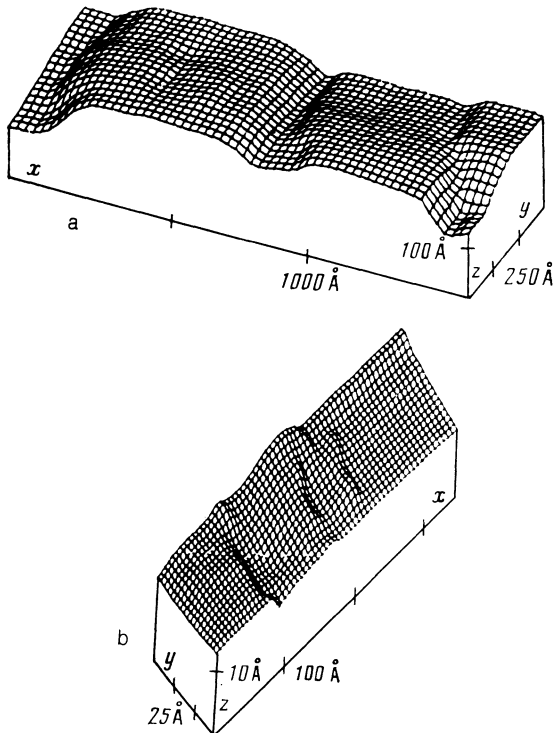


FIG. 1. Typical STM images of bright-dipped (110) tungsten surface.

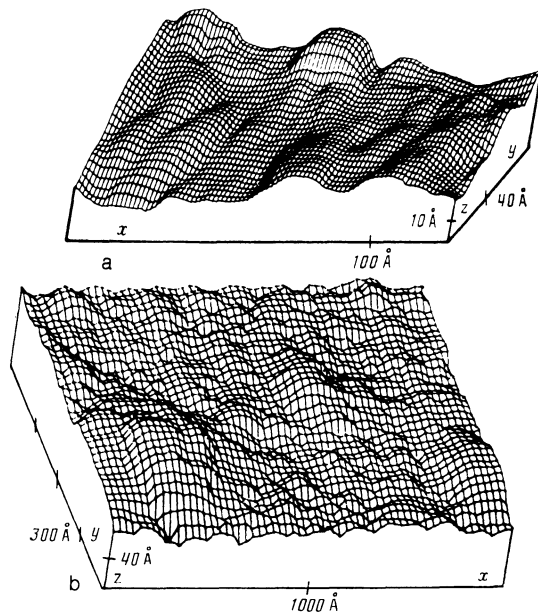


FIG. 2. Typical STM images of bright-dipped (100) tungsten surface.

$$h(x, y) = \sum_{k_x, k_y} \{ F(k_x, k_y) \exp[i(k_x x + k_y y)] \},$$

$$F(k_x, k_y) = \frac{1}{N_x N_y} \sum_{x, y} \{ h(x, y) \exp[-i(k_x x + k_y y)] \},$$

where $h(x, y)$ is the relief of the surface, x and y are the coordinates along the median plane, k_x and k_y are the corresponding wave vectors, and $F(k_x, k_y)$ is the Fourier transform of $h(x, y)$. Assuming that $F(k_x, k_y) = F(|\mathbf{k}|)$, we obtain for the dependence of the two-dimensional Fourier transform on the wave vector the relation $|F(k)| \propto k^{-p}$. The value of p is the same for the (100) and (110) faces within the scatter of the data, and ranges from 1.1 to 1.4.

DISCUSSION

In EF experiments, in view of the finite contact dimension, the electrons recorded as specularly reflected are those traveling in a small solid angle around the normal to the surface. The aperture of this angle is b/l (b is the diameter of the contacts and l is the distance between them), and equals approximately 5° for experiments with tungsten. Thus, the decrease in the probability of specular reflection in the EF data is due to scattering by angles larger than 5° .

Contributions to scattering of electrons reflected from the surface are made by scattering from adsorbed impurities, surface roughnesses, and others. Since the specular-reflection probability measured by the EF is the same for an atomically clean and for a real surface saturated with adsorbed atoms,¹¹ it can be concluded that in the case of a real surface the main contribution to the scattering is made by the surface relief. If it is assumed that the dimension of the roughness along the surface is large enough (compared with the screening radius in the metal and with the STM resolution), the images obtained with an STM will represent the relief from which the electrons are scattered.

The character of scattering by a rough surface depends on the size of the roughnesses. If the roughness dimension L

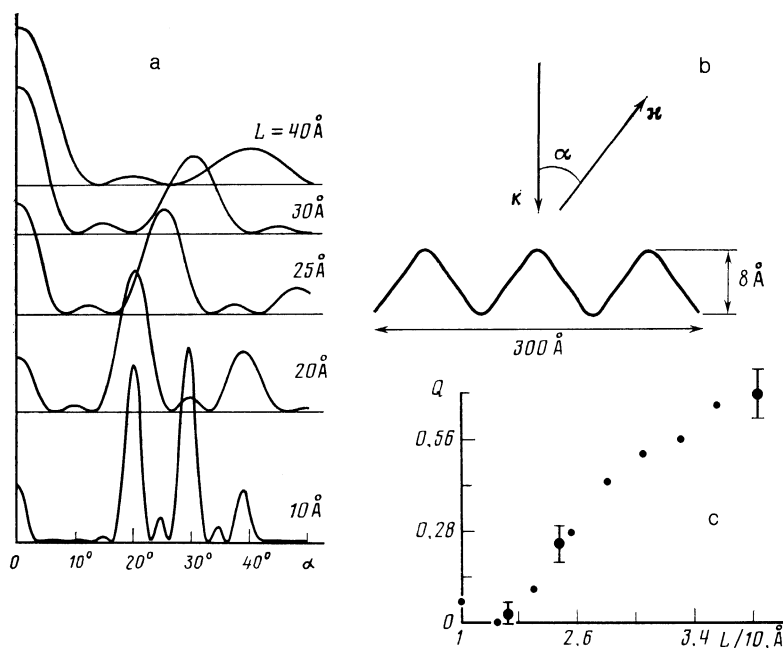


FIG. 3. Results of calculation of the scattering of a plane wave by a one-dimensional relief of triangular shape.

along the surface is much larger than the de Broglie wavelength of the electrons ($L \gg \lambda$), scattering by such a relief is described by specular reflection from a locally plane surface with a normal that deviates from the mean normal. The maximum scattering angle is determined by the maximum deviation of the local normal from its mean direction. In the case $L \sim \lambda$, an important role is assumed by interference effect and the specular-reflection probability should depend on the wavelength.

The presence of large atomically-flat sections on the (110) surface of tungsten agrees with the fact that in EF experiments the specular-reflection probability of the conduction electron is independent of the de Broglie wavelength ($q \approx 0.6$ at $10 \text{ \AA} \ll \lambda \ll 50 \text{ \AA}$, see Ref. 11). The deviation of the specular-reflection probability from unity is apparently due to scattering by the large-scale relief (the drops between the planar sections, see above).

Two possible explanations were offered in Ref. 11 for the dependence of the specular-reflection probability on the electron wavelength in the case of the (100) surface of tungsten: 1) the presence of surface roughness ($L \sim \lambda$); 2) the high probability of umklapp processes on perfect sections of the (100) face. Our data favor the first explanation. Since the (100) surface consists of triangular facets whose normals to the inclined surfaces deviate from the mean normal by $18\text{--}10^\circ$ and whose dimensions along the surface are $50\text{--}200 \text{ \AA}$, the condition $L \gg \lambda$ is satisfied for $\lambda = 10 \text{ \AA}$. Therefore all the electrons will be scattered by $3\text{--}20^\circ$ in different directions from the normal to the median plane, and the probability of specular reflection will be close to zero. Electrons of wavelength $\lambda = 50 \text{ \AA}$ satisfy the condition $L \gg \lambda$ and interference effects are important: since the heights of the facets are several times smaller than the electron wavelength, the scattering indicatrix on reflection will be strongly "elongated" in the direction of the specular reflection, i.e., the specular-reflection coefficient will be large. Just as in the case of the (110) surface, the deviation of the specular-reflection probability from unity for electrons with maximum

wavelength is apparently due to scattering by the large-scale relief ($L \gg \lambda$).

To illustrate the foregoing arguments, we calculated the angular distribution of the intensity of plane-wave scattering by a one-dimensional relief of triangular form (Fig. 3b). The tangent-plane approximation was used in the calculation (Fig. 3b). In this case the amplitude of the scattered wave is

$$U(\mathbf{k}, \boldsymbol{\kappa}) = A \int_{s_0} \exp\{-i[\mathbf{q}\mathbf{r} + q_z h(\mathbf{r})]\} (q_z - \mathbf{q}\boldsymbol{\gamma}) d\mathbf{r},$$

where $U(\mathbf{k}, \boldsymbol{\kappa})$ is the amplitude of the scattered wave, \mathbf{k} the wave vector of the incident wave, $\boldsymbol{\kappa}$ the wave vector of the reflected wave, $\mathbf{q} = \boldsymbol{\kappa} - \mathbf{k}$, $\boldsymbol{\gamma} = \nabla h(\mathbf{r})$, and $h(\mathbf{r})$ the surface relief. For the method to be valid it is necessary that the curvature radius of the surface at each point be much larger than the wavelength. For the relief observed in our study this condition is approximately satisfied. The calculation result is given in Fig. 3a, which shows the dependences of the scattering intensity on the angle between the reflection direction and the mean normal to the surface for several wavelengths. The peaks on the plot of the scattering intensity vs the angle for $\lambda = 10 \text{ \AA}$ (Fig. 3a) near $20\text{--}30$ degrees correspond to specular reflection from the inclined sections of the relief (Fig. 3b). With increase of wavelength, the amplitudes of these peaks decrease, and at the same time the amplitude of the specular peak increases. Figure 3c shows the dependence of the specular reflection probability on the wavelength for a model calculation, and also experimental EF data.¹¹ The specular-reflection probabilities were taken to be the ratios of the fraction of electrons emitted in directions with $\alpha < 5^\circ$ (Fig. 3b) to the total number of electrons. As seen from the figure, a simplified calculation (without allowance for the shape of the Fermi surface and for the two-dimensional character of the roughnesses permits a satisfactory reconciliation of the features of the relief with the measured dependence of q on λ .

Thus, the dependence, on the de Broglie wavelength, of the probability of specular reflection of conduction electrons

normally incident on the (100) face of tungsten can be attributed to scattering by the facets, and the high probability of the specular reflection of all groups of electrons incident on the (110) face is due to the presence of large atomically flat sections.

The obtained form of the Fourier spectrum of the surface indicates that the real reliefs of the surfaces (100) and (110) does not have a random Gaussian character. To describe the roughness of a surface and the associated processes we must know not only the mean squared deviation $(\Delta h^2)^{1/2}$ and the average dimension of the roughnesses along the surface, but also the shapes of the roughnesses.

The authors thank S. I. Bozhko and A. A. Moskalev for technical help.

¹⁾It was established by EF experiments that the character of the conduction-electron reflection from the surface is the same for different tungsten samples having the same orientation and prepared by the same method, and remains unchanged for a long time (more than five years).

¹⁾V. S. Tsoi, *Pis'ma Zh. Eksp. Teor. Fiz.* **19**, 114 (1974) [*JETP Lett.* **19**, 70 (1974)].

- ²V. S. Tsoi and I. I. Razgonov, *ibid.* **25**, 30 (1977) [**25**, 26 (1977)].
³V. S. Tsoi, J. Bass, P. A. M. Benistant, *et al.*, *J. Phys.* **F9**, L221 (1979).
⁴H. Sato and F. Kimura, *ibid.* **14**, 1905 (1984).
⁵P. A. M. Benistant, H. van Kempen, and P. Wyder, *ibid.* **F15**, 2445 (1985).
⁶V. S. Tsoi and V. I. Razgonov, *Pis'ma Zh. Eksp. Teor. Fiz.* **23**, 107 (1968) [*JETP Lett.* **92** (1968)].
⁷V. G. Peschanskiĭ and M. Ya. Azbel, *Zh. Eksp. Teor. Fiz.* **55**, 1980 (1968) [*Sov. Phys. JETP* **28**, 1045 (1969)].
⁸P. P. Lutsishin, O. A. Panchenko, and A. A. Kharlamov, *ibid.* **64**, 2148 (1973) [**37**, 1083 (1973)].
⁹O. A. Panchenko, A. A. Kharlamov, and Yu. G. Ptushinskii, *ibid.* **67**, 780 (1974) [**40**, 386 (1974)].
¹⁰S. I. Bozhko, A. A. Mitryaev, O. A. Panchenko, *et al.*, *Fiz. Nizk. Temp.* **5**, 739 (1979) [*Sov. J. Low Temp. Phys.* **5**, 351 (1979)].
¹¹V. S. Tsoi and I. I. Razgonov, *Zh. Eksp. Teor. Fiz.* **74**, 1137 (1978) [*Sov. Phys. JETP* **47**, 597 (1978)].
¹²G. Binning and H. Rohrer, *IBM J. Res. Dev.* **30**, 355 (1986).
¹³A. M. Baro, R. Miranda, J. Alaman, *et al.*, *Nature* **315**, 253 (1985).
¹⁴M. S. Khaikin, A. M. Troyanovskii, V. S. Edel'man, *et al.*, *Pis'ma Zh. Eksp. Teor. Fiz.* **44**, 193 (1986) [*JETP Lett.* **44**, 245 (1986)].
¹⁵P. A. M. Benistant, C. F. A. van de Walle, and H. van Kempen, and P. Wyder, *Phys. Rev.* **B33**, 690 (1986).
¹⁶P. K. Hansma, *J. Appl. Phys.* **61**(2), R1 (1986).
¹⁷C. F. A. van de Walle, J. W. Gerristen, H. van Kempen, and P. Wyder, *Rev. Sci. Instrum.* **56**, 1573 (1985).
¹⁸F. G. Bass and I. M. Fuks, *Wave Scattering by a Statistically Rough Surface* [in Russian], Nauka, 183 (1972).

Translated by J. G. Adashko